PERGAMON

Deep-Sea Research I 49 (2002) 1141–1164

DEEP-SEA RESEARCH
PART I

www.elsevier.com/locate/dsr

A view of ACC fronts in streamfunction space

Che Sun[a,*], D. Randolph Watts[b]

[a] *Geophysical Fluid Dynamics Laboratory/NOAA, Princeton University, P.O. Box 308, Princeton 08542, USA*
[b] *Graduate School of Oceanography, University of Rhode Island, Narragansett, USA*

Received 4 April 2001; received in revised form 14 December 2001; accepted 17 April 2002

Abstract

The fronts and water masses in the Antarctic Circumpolar Current (ACC) are examined with a streamfunction projection of historical hydrographic data. The study shows that only structural criterion provides circumpolarly consistent and time-invariant definition for ACC fronts. The Polar Front position varies little in the streamfunction space, but the Subantarctic Front exhibits significant meridional deflection. Two types of the Antarctic Intermediate Water (AAIW) are identified: the Pacific-Atlantic type represents the recently-formed AAIW through the along-isopycnal subduction of polar surface waters; the Indian–Australian type represents relatively old AAIW which is strongly modified by the Agulhas water. The Subantarctic Mode Water (SAMW) is located in the South Pacific and south of Australia. There is evidence that the SAMW in the southeast Pacific originates from polar surface waters. Therefore the eastward freshening and cooling of SAMW is ascribed to influences from the south.

Keywords: Hydrography; Streamfunction projection; ACC fronts; AAIW; SAMW

1. Introduction

The Antarctic Circumpolar Current (ACC) is characterized by two conspicuous fronts, the Subantarctic Front (SAF) and the Polar Front (PF). Between them is a transition zone called the Polar Front Zone (PFZ). Fig. 1 shows a typical ACC transect along the WOCE SR3 line south of Australia. Both temperature and salinity fields display a variety of hydrographic features ranging from small-scale intrusions to a large-scale low-salinity tongue.

Observational studies in the Southern Ocean often rely on individual hydrographic surveys. These Eulerian descriptions are complicated by the great variability in the region. Limited horizontal resolution because of time constraints in achieving a synoptic survey also poses a problem. Despite efforts to describe the large-scale ACC system (e.g., Piola and Georgi, 1982; hereafter PG82 Orsi et al., 1995, hereafter O95; Belkin and Gordon, 1996, hereafter BG96), our knowledge of ACC fronts and frontal water masses (intermediate water and mode water) is still fragmentary and sometimes conflicting.

A new method called the circumpolar gravest empirical mode (GEM) (Sun and Watts, 2001,

*Corresponding author.
E-mail address: cns@gfdl.noaa.gov (C. Sun).

0967-0637/02/$ - see front matter
PII: S0967-0637(02)00027-4

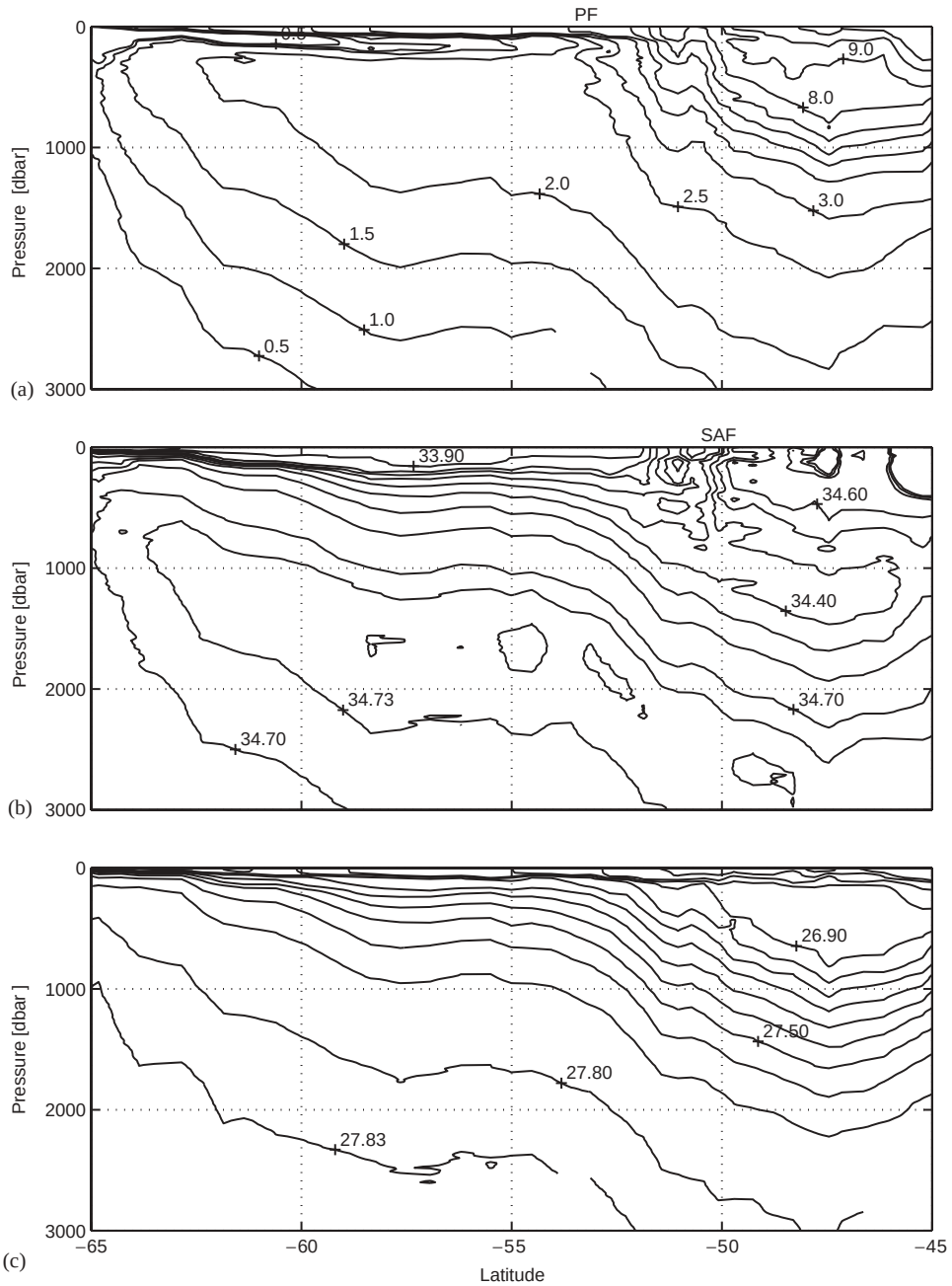

Fig. 1. A typical hydrographic section across the ACC south of Australia: (a) temperature (°C), (b) salinity and (c) potential density ($kg\,m^{-3}$).

hereafter SW2001) has been developed and is applied here. By projecting hydrographic data into a baroclinic streamfunction space, the method removes most of the temporal variability associated with mesoscale eddies and meandering fronts, and is able to utilize all historical casts in

the Southern Ocean. The projection is equivalent to a streamfunction mean field (Sun and Watts, 2002).

The circumpolar GEM fields are parameterized by geopotential height, pressure and longitude, capturing more than 97% of the subsurface density and temperature variance in the ACC region. The GEM dominance implies that thermohaline fields are nearly rigid in streamfunction space, revealing a new aspect of the ACC structure. A theoretical explanation can be made by extending the Taylor–Proudman theorem to inhomogeneous fluids (Sun, 2001).

Figs. 2 and 3 show the cross-stream sections of circumpolar GEM fields at 140° E (close to the SR3 line) and 90° W (in the southeast Pacific). The streamfunction parameter is geopotential height

$$\phi_{1000} = \int_{100}^{1000} \delta \, \mathrm{d}p,$$

where δ is specific volume anomaly. Potential vorticity (planetary part) is defined as

$$\mathrm{PV} = \frac{f}{\rho_0} \frac{\partial \sigma_\theta}{\partial z},$$

where f is the Coriolis parameter and σ_θ is potential density relative to the surface. The GEM as a streamfunction mean field smooths over intrusions and other transient features, but retains all the characteristic hydrographic features that appear repeatedly in the streamfunction space.

We will examine the circumpolar variation of the ACC frontal system by taking a series of cross-stream section views, along-stream views, core layer views, and plan views of the circumpolar GEM fields. Such a tomographic analysis is necessary because ACC water masses exhibit large circumpolar variation and can not be described on a single isobaric or isopycnal surface. Compared with traditional geographic studies, the streamfunction approach avoids the complication of topography and enables us to focus more on the water mass itself. It has particular advantage in regions where different frontal systems come close or even merge together (such as in the Agulhas Retroflection), and therefore gives a better description of frontal water masses in their source regions.

2. ACC fronts

2.1. Front definition

Oceanic fronts are generated by a variety of mechanisms, including Ekman convergence, water mass boundary, coastal upwelling, convergent mean flow, and tidal stirring. Gill (1982) described each type of front in detail. He pointed out that water mass boundary fronts, such as those separating the subarctic and subtropical gyres in the North Pacific, are distinct in temperature and salinity sections but not in density sections.

The ACC has a meridional width more than 1000 km and separates subtropical waters from Antarctic waters. The SAF and the PF are water mass boundary fronts embedded in this broad baroclinic current. There is debate on how to identify ACC fronts in an environment of great spatio-temporal variability. The many definitions fall into three categories:

(1) *Structural criteria*: Observations indicate that ACC fronts are continuous circumpolar phenomena. Across each front there is a distinct change of vertical thermohaline structure: the PF is the northern terminus of the near-surface temperature inversion layer, and the SAF is the beginning of the salinity minimum layer. These phenomenological characters provide a definition of ACC fronts in terms of structural criteria, which are consistent around Antarctica, and reflect the baroclinic nature of the current (BG96).

(2) *Scalar criteria*: Structural criteria may not be quantitatively applicable in a synoptic survey due to lack of horizontal resolution and complications of mesoscale variability. To locate a front, oceanographers often look for a particular isotherm or isohaline at a certain depth based on past experience (see BG96 for a list of scalar criteria). Different thermohaline indicators may give different frontal positions, and few of them apply to the entire

Southern Ocean because of water mass variation. To address this problem, BG96 used a "parameter-longitude" scheme that allows the prescribed T–S criterion to be gradually modified downstream.

(3) *Gradient criteria*: On a synoptic transect, large isopycnal (or isotherm) tilt is associated with enhanced horizontal gradients and represents a baroclinic jet (local transport maximum or frontal filament). The concentrated isopycnal

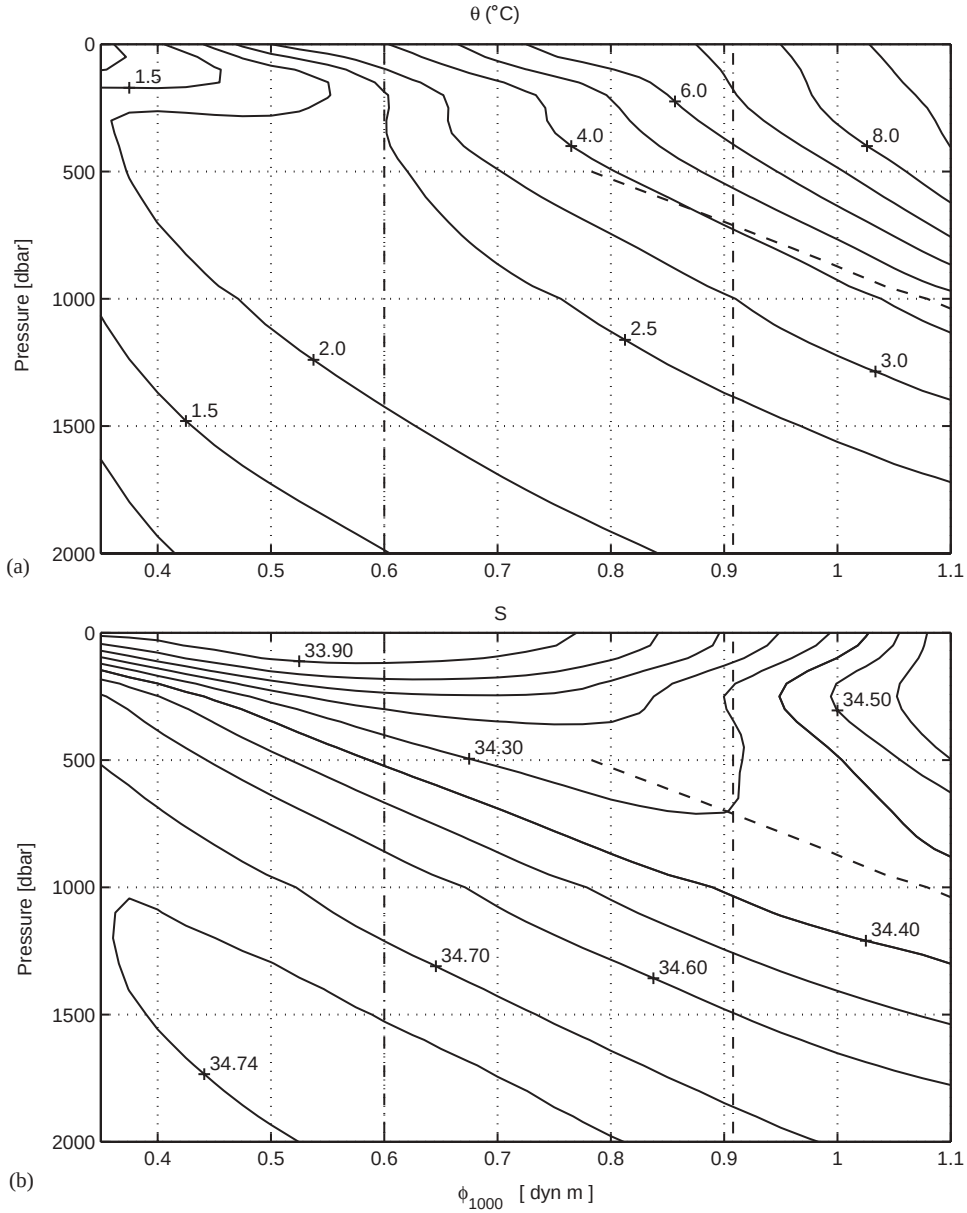

Fig. 2. Cross-stream section view of GEM fields at 140° E south of Australia. The vertical dash-dotted lines from left to right represent the PF and the SAF. The dashed curve is the potential density surface (27.22 kg m^{-3}) at the salinity minimum core: (a) potential temperature, (b) salinity, (c) oxygen, and (d) potential vorticity in the cold season.

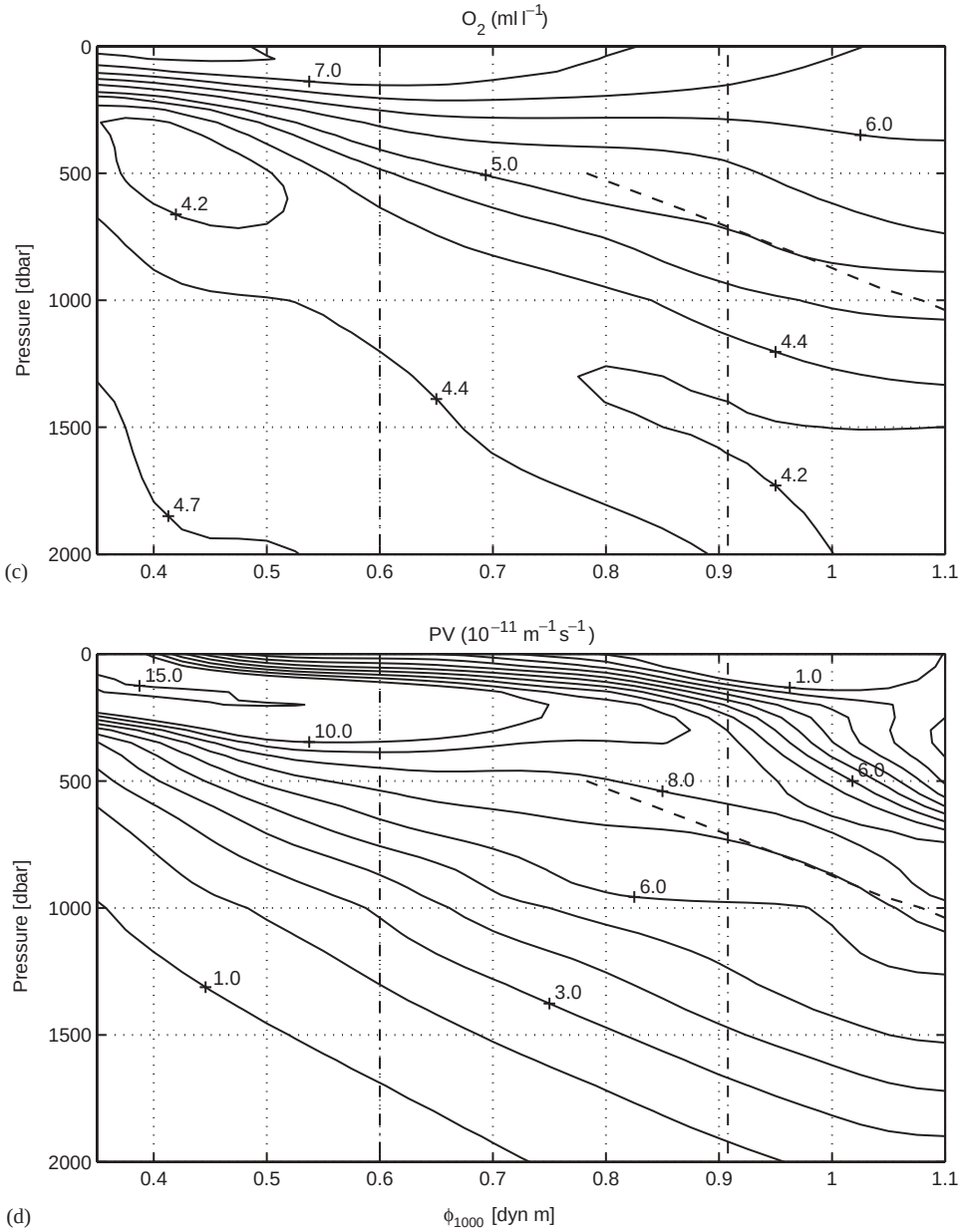

Fig. 2 (*continued*).

tilt is used by some investigators as the principal indicator of the ACC fronts (e.g., O95). The approach is problematic because a gradient field varies strongly in response to mesoscale eddies and topographic effects. At the SR3 line, the SAF and the PF tend to form a broad baroclinic zone on the northern flank of the Southeast Indian Ridge (Fig. 1), rather than the step-like filaments observed at the Drake Passage (Nowlin et al., 1977).

2.2. Streamfunction approach

Identifying fronts in geographic space is complicated by the spatio-temporal variability of the ACC. For example, a hydrographic transect across an S-shaped meander in the SAF, which spans 300 km meridionally at the SR3 line (see Fig. 9 in Watts et al., 2001), may lead to a conclusion that

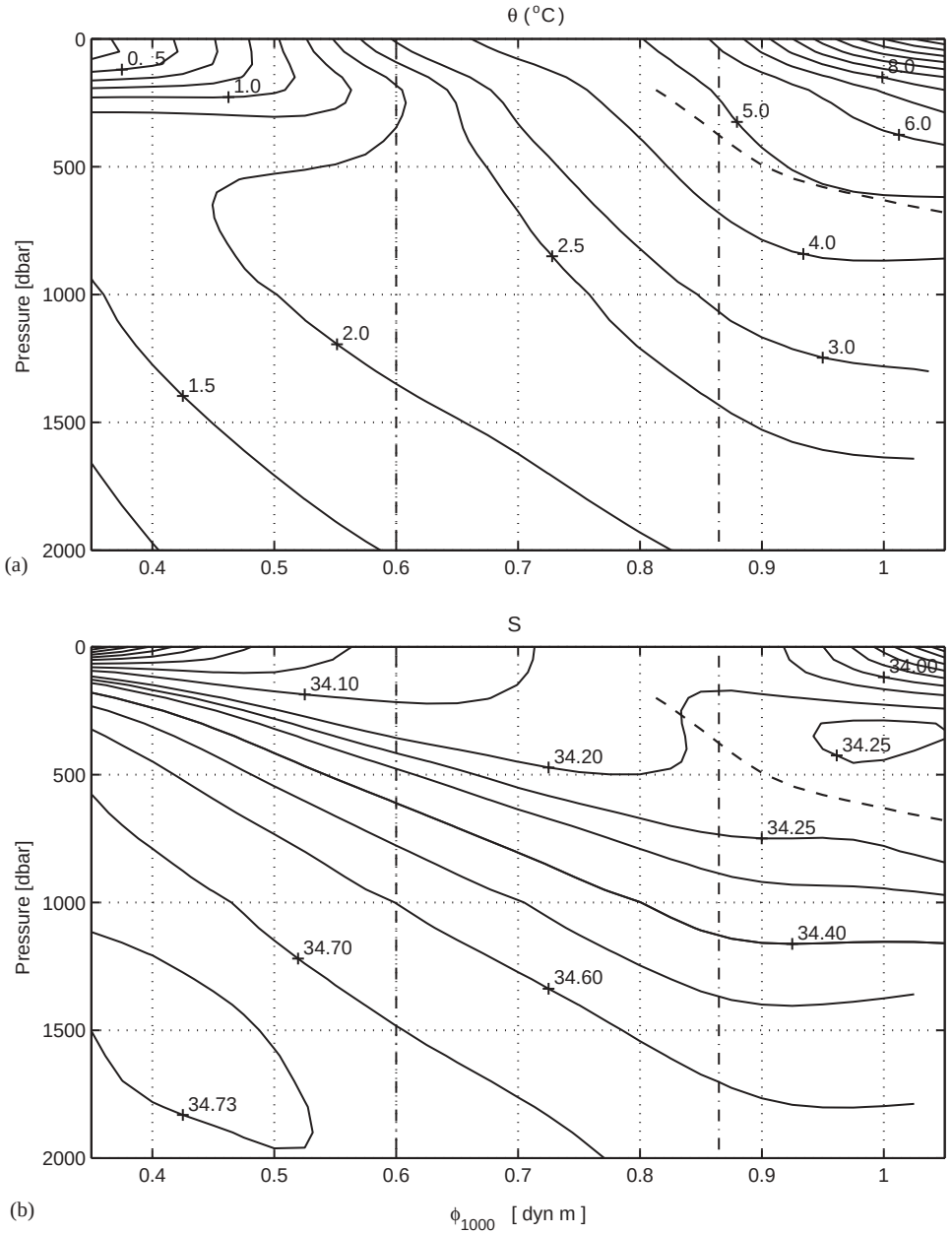

Fig. 3. Same as in Fig. 2 except for GEM fields at 90°W in the southeast Pacific. The dashed curve is the potential density surface (27.08 kg m^{-3}) at the salinity minimum core: (a) potential temperature, (b) salinity, (c) oxygen, and (d) potential vorticity in the cold season.

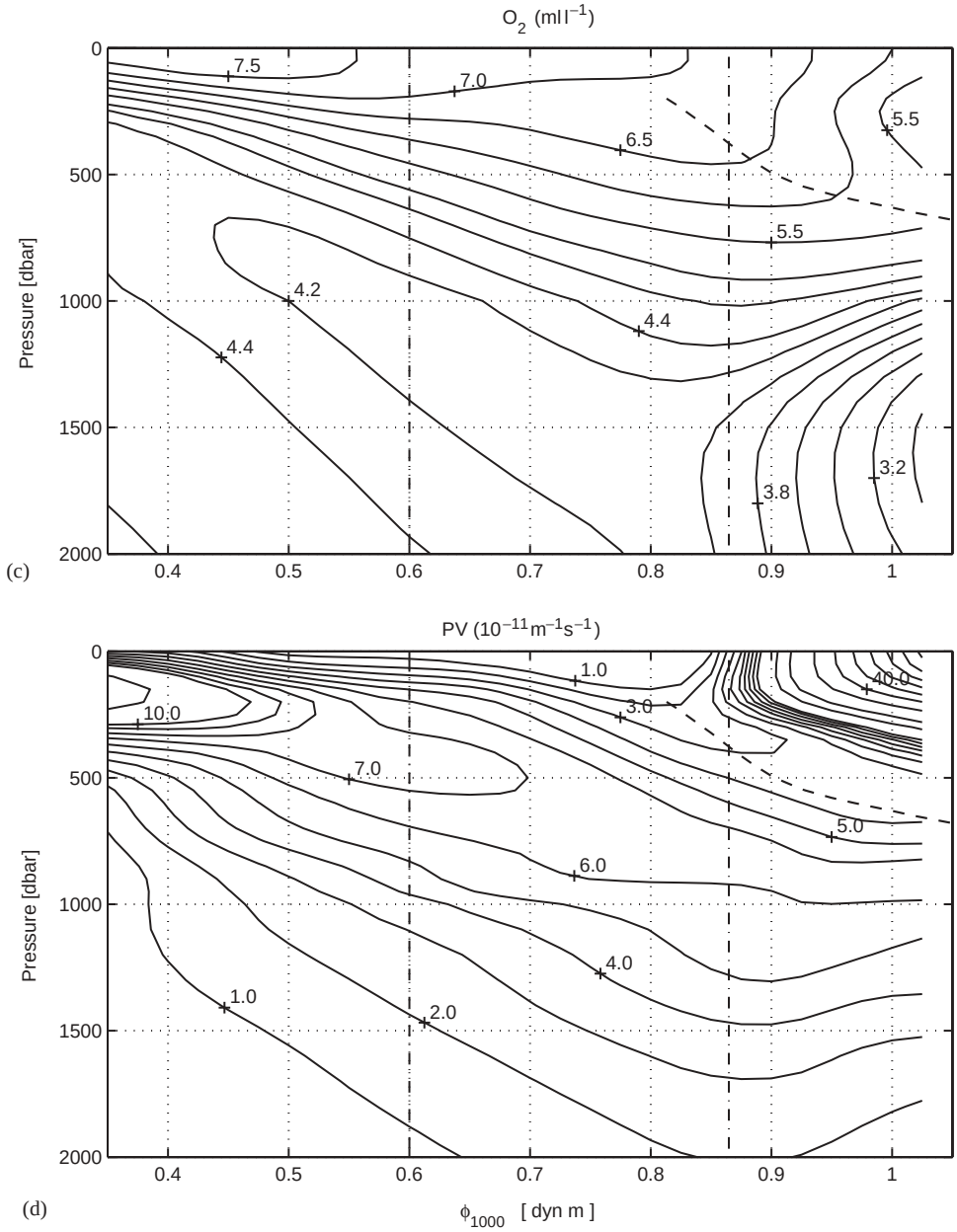

Fig. 3 (*continued*).

there are two SAF branches, especially if the survey has insufficient resolution.

As a remedy, projecting data into a baroclinic streamfunction space removes most of the variability associated with geostrophic advection (SW2001). Because each streamfunction value corresponds to a fixed vertical profile in a streamfunction-mean field, the dominant GEM field keeps all hydrographic information pertinent to a structural criterion, which is based on the

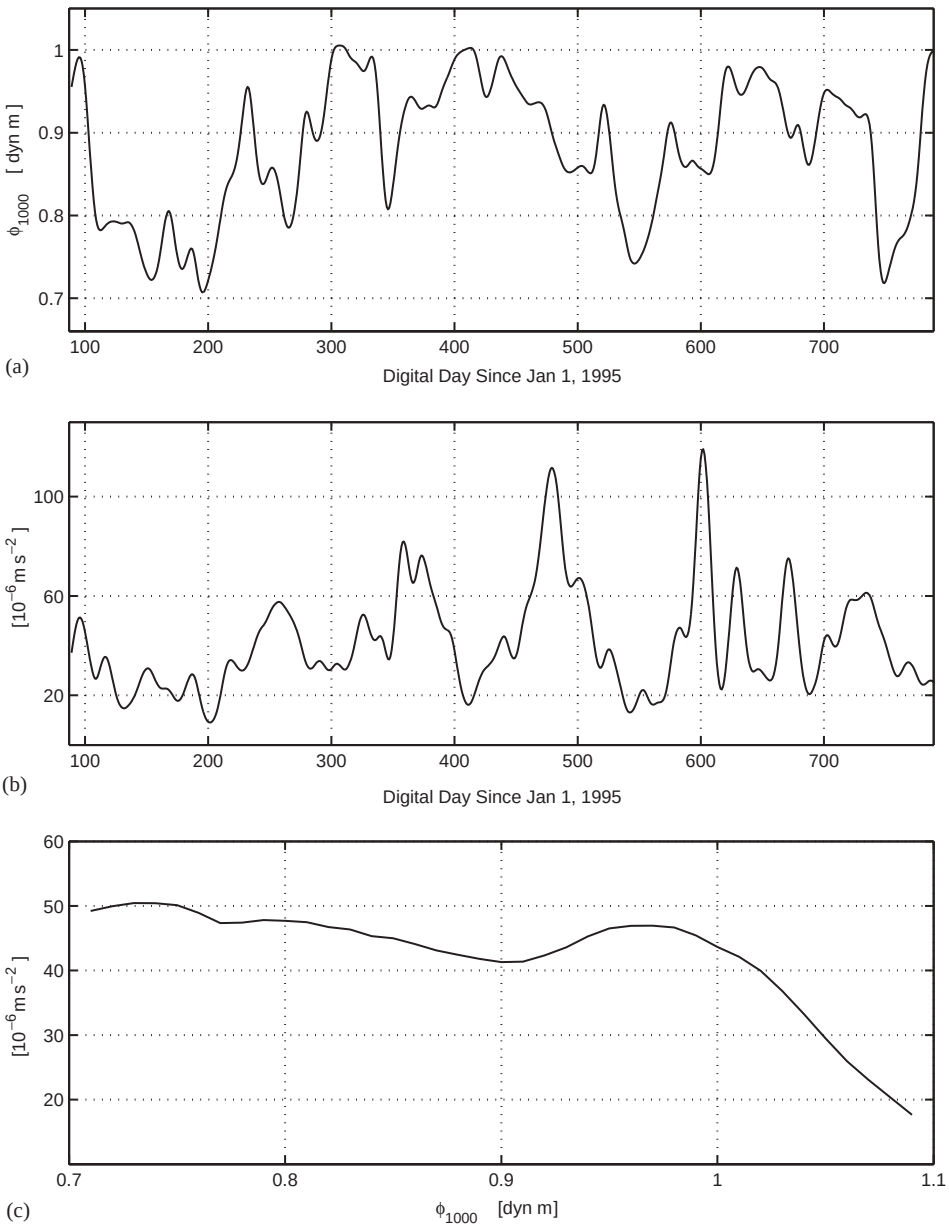

Fig. 4. The SAFDE experiment: (a) geopotential value at the axis of the baroclinic jet; (b) lateral geopotential gradient at $\phi_{1000} = 0.9$ dyn m, and (c) 2-year mean of lateral geopotential gradient at each ϕ_{1000}.

change of vertical structure across the front. The quantitative applicability of a structural criterion is further ensured by the high horizontal resolution of a streamfunction mean field, which is built on all historical data including non-synoptic surveys.

An ideal definition of the ACC front should be circumpolarly consistent and to a certain extent time-invariant. The application of structural criteria in streamfunction space has these characteristics, but scalar criteria and gradient criteria do not.

Two-year mooring observations at the SR3 line during the Subantarctic Flux and Dynamics Experiment (SAFDE) (a detailed description given in Watts et al., 2001) shed more light on the relation between different criteria. In that study, acoustic travel time (from surface to bottom) measured by an array of inverted echo sounders was converted into geopotential height through a GEM correlation. Horizontal geopotential gradient is then calculated from an objective interpolation. Results showed: the baroclinic jet does not correspond to a particular streamfunction contour (Fig. 4a); a front defined by the structural criterion in streamfunction space, which corresponds to one streamfunction value at the SR3 line, is not always accompanied by large isopycnal tilt (Fig. 4b); in the statistical sense, there is likely a correspondence between the baroclinic jet and the front defined by a structural criterion (Fig. 4c, note the small peak at $\phi_{1000} = 0.95$ dyn m).

2.3. Identification of ACC fronts in GEM fields

(1) *Polar Front*: To identify the PF in the circumpolar GEM fields, we look for the subsurface temperature inversion layer (Fig. 5). Its northern terminus, which sinks through 200–400 dbar, is the location of the PF (a structural criterion used by Peterson and Whitworth, 1989). The variation of PF position is relatively small (0.6 ± 0.05 dyn m). Fig. 5 also shows a shallow cold tongue emanating from the Antarctic coast in the southeast Pacific (100° W) and intruding into the Drake Passage.

In situ observations in the Drake Passage (Sievers and Nowlin, 1984), in the Western Scotia Sea (Gordon et al., 1977) and south of Australia (Rintoul et al., 1997) show that the PF axis is always around the ϕ_{1000} value of 0.6 dyn m. Different authors used different pressure ranges for their geopotential height calculations, but the values are interchangeable through the GEM fields.

(2) *Subantarctic Front*: In a meridional section, the SAF is the place where the salinity minimum layer rapidly descends to 400–600 m depth (Whitworth and Nowlin, 1987). Our algorithm searches for the salinity minimum layer in the water below 400 m (Fig. 6). Its southernmost limit is the location of the SAF (dash-dotted curve). The geopotential height values at the SAF range from 0.8 dyn m in the southwest Atlantic to 0.95 dyn m south of New Zealand.

SW2001 chose ϕ_{1000} as the streamfunction parameter in order to utilize the extensive set of hydrographic casts that only reached 1000 dbar. The frontal pattern will change if we switch to a different streamfunction parameter, for example, the mass transport function relative to 3000 dbar

$$\Psi_{3000} = \int_0^{3000} \frac{p\delta}{g}\,\mathrm{d}p.$$

Fig. 7 is obtained by a simple interpolation of GEM fields. It may be tempting to infer a cross-SAF transport of 30 Sv from the figure, which should not be the case because the SAF is a near-surface feature (along-isopycnal thermohaline gradients disappear below the intermediate water level). Its meridional deflection in streamfunction space reflects the modification by different subantarctic surface waters along the ACC, rather than the mass transport across a material surface. Because of a lack of data over the Campbell Plateau, not all the subantarctic water mass (up to $\Psi_{3000} = 280 \times 10^5$ J m^{-2} from Fig. 2 in Sun and Watts, in press) is represented in the GEM fields south of New Zealand. The missing part may balance the Indonesian throughflow.

2.4. Compare with property criteria

The frontal properties derived from GEM fields using structural criteria should be comparable to those scalar criteria applied in synoptic surveys.

Fig. 8a shows the surface temperature along the SAF axis, agreeing with Burling's (1961) criterion of $T_0 = 8$°C in the ACC south of New Zealand (his studied region). Peterson and Whitworth (1989) identified the SAF in the southwestern Atlantic by isotherms of 4–5°C at the 200 m depth,

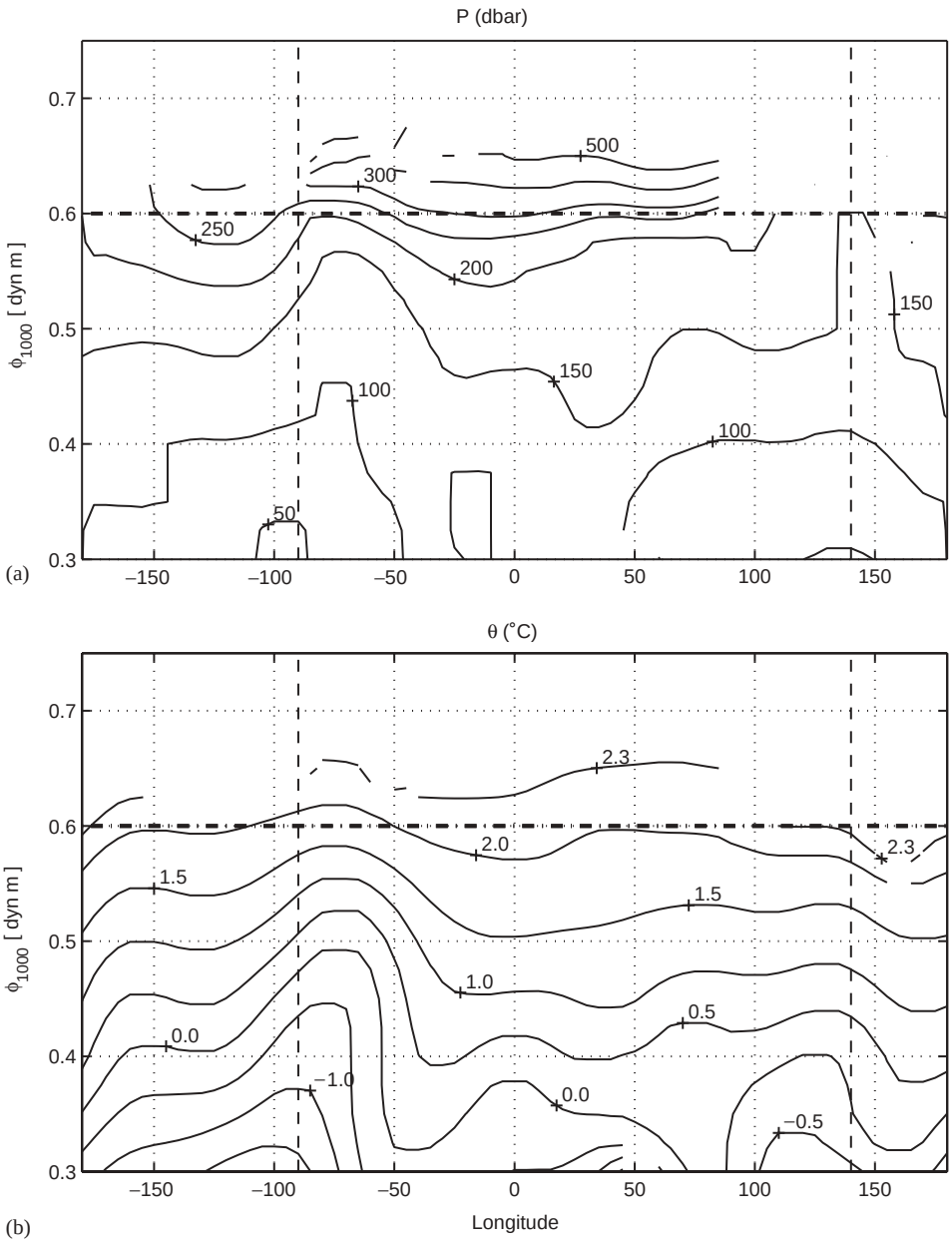

Fig. 5. Core layer view of the subsurface temperature minimum layer: (a) pressure, and (b) potential temperature. The PF axis is represented by the dash-dotted line. The dashlines correspond to the longitudes of two sections in Figs. 2 and 3.

which agrees with Fig. 8b. The agreement with traditional criteria in their intended regions suggests that applying a structural criterion in streamfunction space is appropriate. On the other hand, we confirm that there is no scalar criterion suitable for locating the SAF in all parts of the ACC.

Along the PF axis, the temperature at 200 dbar (Fig. 8c) varies from 1.8°C at the Drake Passage to 2.6°C south of Tasmania, slightly deviating from

the criterion of $T_{200} = 2^{\circ}C$ used by O95. At the 200 m depth, both the SAF and the PF warm up in the southwest Atlantic and the South Indian Ocean and cool off in the South Pacific, consistent with the variation of ACC heat transport in Sun and Watts (in press).

The front tracking results may be transcribed to geographic space via a mean streamline map

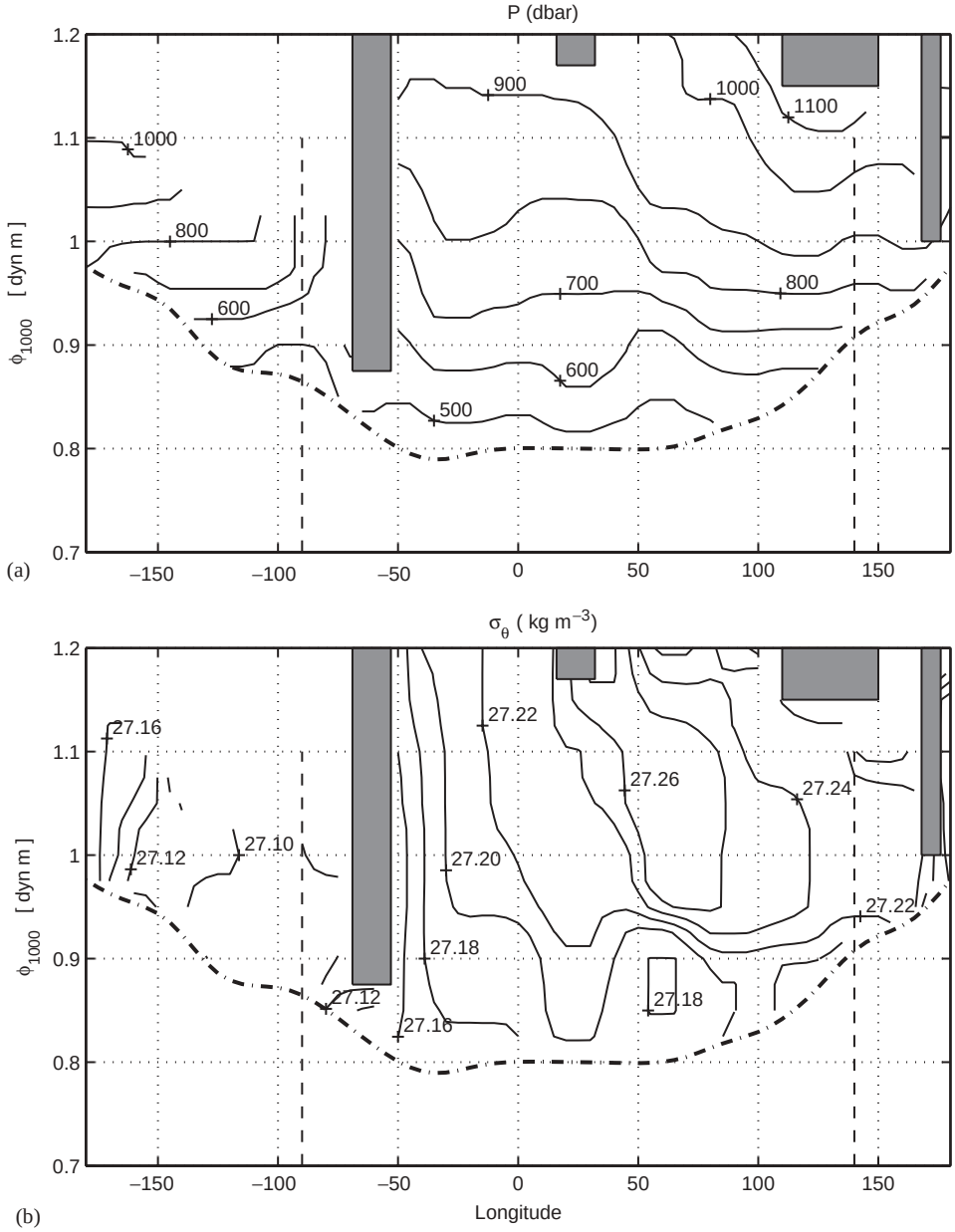

Fig. 6. Core layer view of the salinity minimum layer: (a) pressure, (b) potential density, (c) salinity, (d) potential temperature, (e) oxygen, and (f) potential vorticity. The SAF axis is represented by the dash-dotted curve. The shaded areas from left to right represent South America, South Africa, Australia and New Zealand.

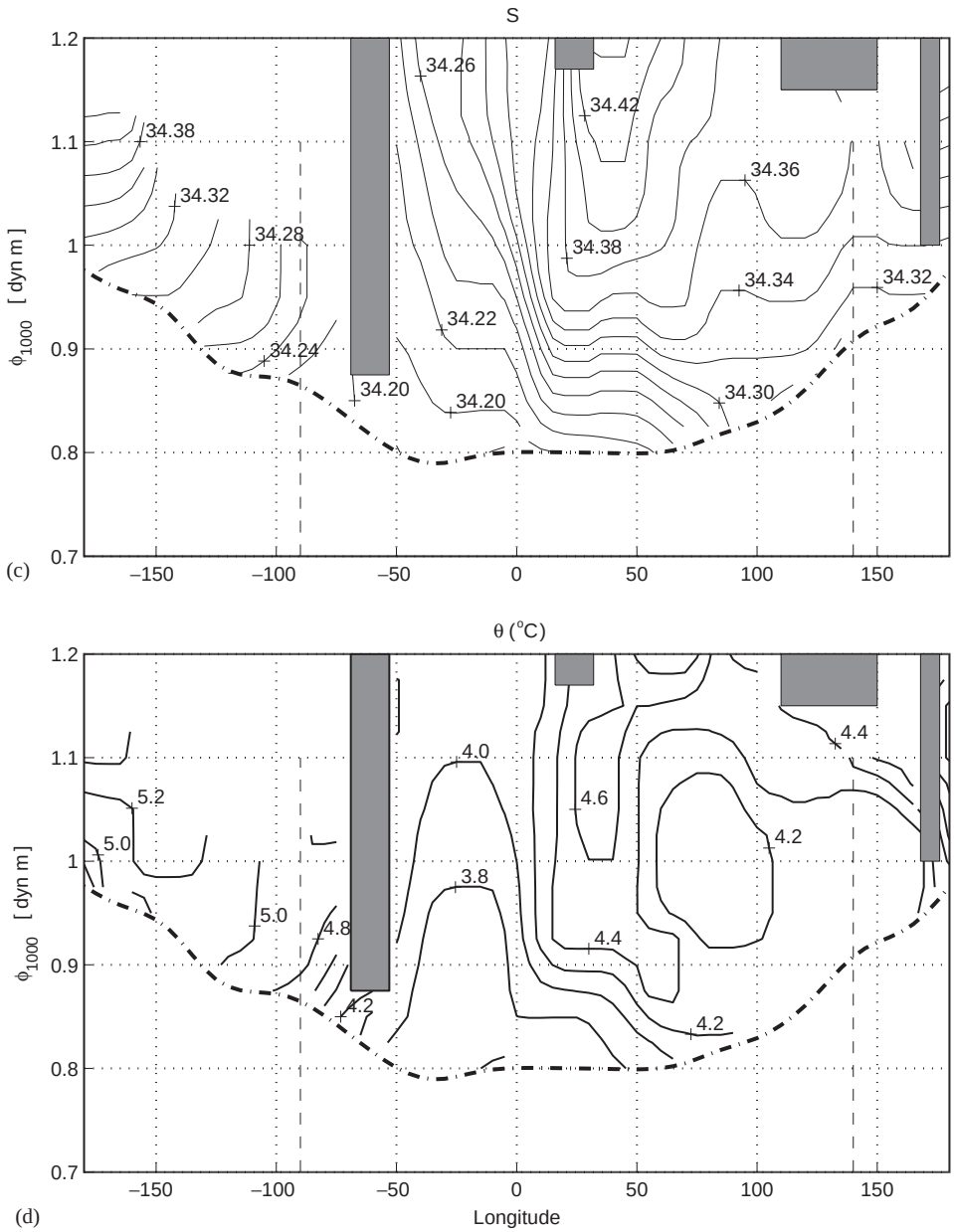

Fig. 6 (*continued*).

(Fig. 9). Many features look familiar (see Fig. 5 in BG96): at the Pacific-Antarctic Ridge (140° W), the PF crosses through the Udintsev Fracture Zone, and the SAF crosses through the Eltanin Fracture Zone; in the Indian Ocean sector, the SAF is deflected to the northern side of the Crozet Plateau (40°E), and the PF is deflected to the northern flank of the Kerguelen Plateau (70°E).

To represent a front by a single line is idealistic, and we do expect some uncertainty

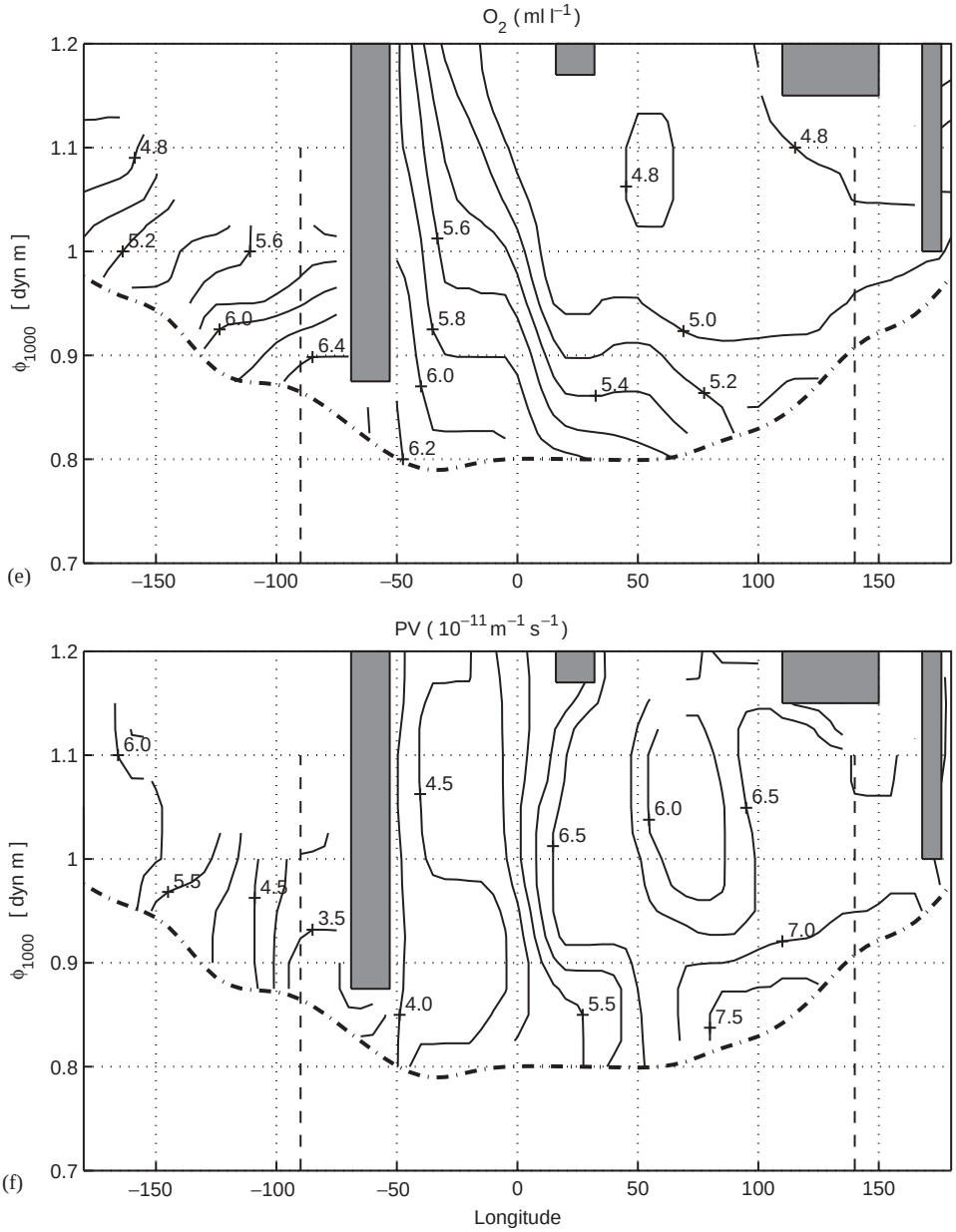

Fig. 6 (*continued*).

in the streamfunction approach. Nevertheless, an important part of the study is to examine the evolution of frontal water masses in their source regions. Using structural criteria allows us to accurately locate their southern limit.

3. Antarctic intermediate water

3.1. Circumpolar distribution

The AAIW in the Southern Ocean is identified by a low-salinity tongue descending across the

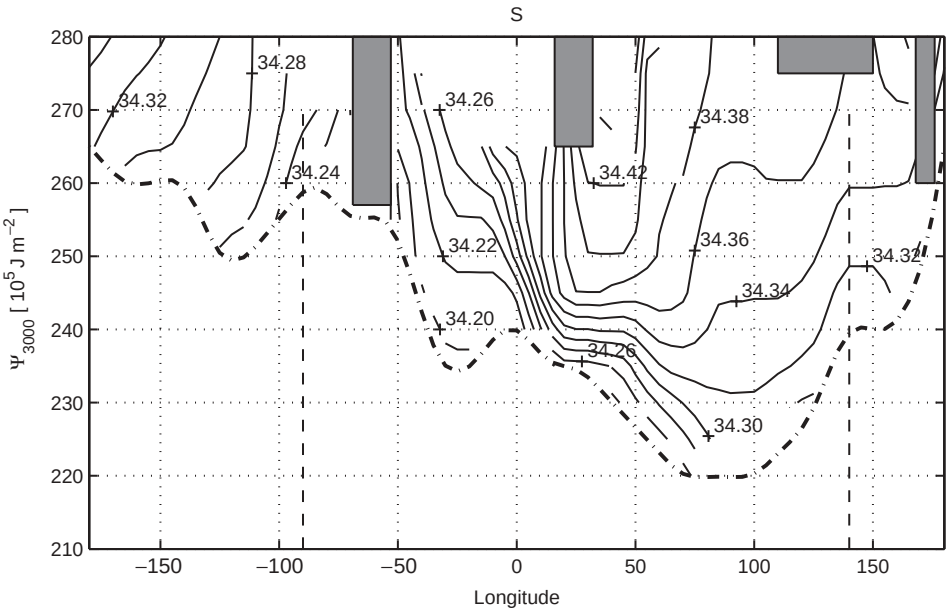

Fig. 7. Core layer view of the salinity minimum layer in the mass transport function coordinates.

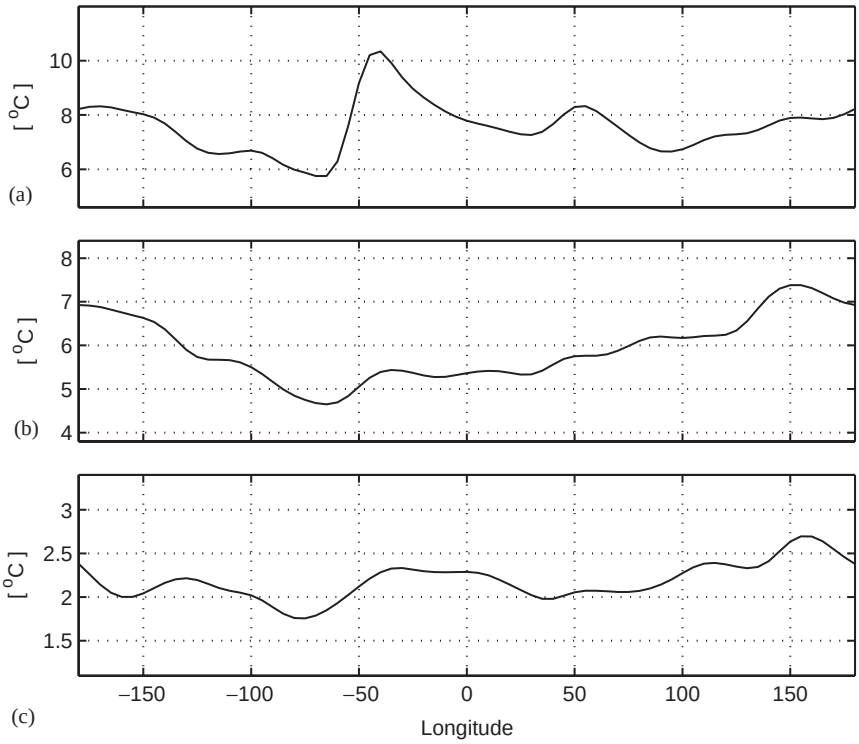

Fig. 8. (a) T_0 along the SAF axis, (b) T_{200} along the SAF axis, and (c) T_{200} along the PF axis.

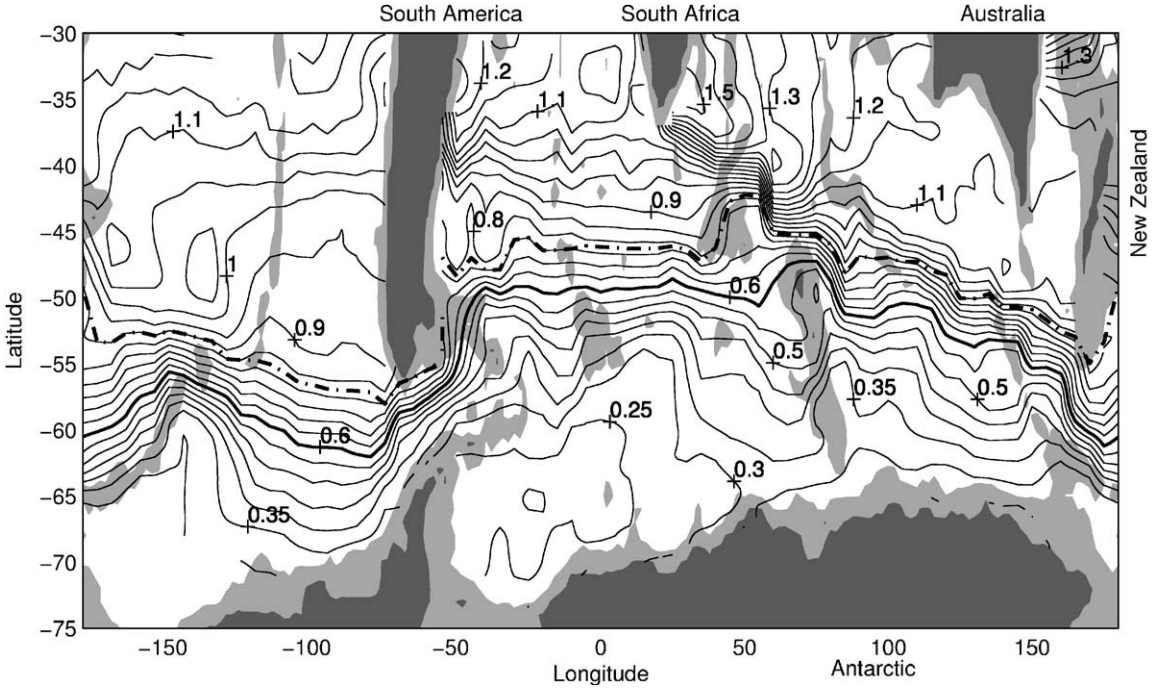

Fig. 9. Geographic plan view: mean streamline map for ϕ_{1000} where the dash-dotted line represents the SAF and the thick solid line represents the PF.

SAF to the Subantarctic Zone. Although a salinity minimum layer is found throughout the Southern Ocean, it does not represent a single water mass zonally advected by the ACC. In various basins it consists of different waters. Figs. 2 and 3 give an illustration: south of Australia (140° E) the AAIW core sits on the $27.22\,\mathrm{kg\,m^{-3}}$ isopycnal and its upper half corresponds to a PV-maximum tongue; in the southeast Pacific (90°W) the core sits on a shallower density surface ($27.08\,\mathrm{kg\,m^{-3}}$) with its upper half corresponding to a PV-minimum tongue. The Pacific AAIW clearly is not the old intermediate water advected from the west, which still sits on a deeper density surface. It essentially represents new formation from polar sources, as discussed later.

The thermohaline distribution at the core of the salinity minimum layer (Fig. 6) shows two distinct types of intermediate water: the AAIW in the South Pacific and the southwest Atlantic is relatively light and fresh, with higher dissolved oxygen and lower PV ($\sigma_\theta < 27.2\,\mathrm{kg\,m^{-3}}$, $S < 34.3$, $O_2 > 5.2\,\mathrm{ml\,l^{-1}}$); the AAIW in the South Indian Ocean and south of Australia is opposite ($\sigma_\theta > 27.2\,\mathrm{kg\,m^{-3}}$, $S > 34.3$, $O_2 < 5.2\,\mathrm{ml\,l^{-1}}$). They are separated by abrupt transitions south of Africa (20°E) and south of New Zealand (170°E), consistent with the geographic analysis by PG82.

The Pacific-Atlantic type of AAIW is centered near the Drake Passage. Its low-salinity tongue is accompanied by a PV-minimum layer and an oxygen-maximum layer, both descending from the PFZ and suggesting a subduction of polar surface waters from the south (the pattern in Fig. 3 also appears in other meridional sections between 120°W and 30°W). The property distribution in the Indian–Australia type of AAIW, on the other hand, reflects the influence of the saline and oxygen-poor Agulhas water from the north.

Divided by the Drake Passage, the intermediate water in the southwest Atlantic is colder, fresher and denser than its Pacific counterpart, a phenomenon noticed by many other investigators (Georgi, 1979; PG82; Talley, 1996).

3.2. Formation mechanism

The comparison between the two types of intermediate water supports the consensus that AAIW is renewed primarily in regions near South America. The current debate is on the source water and the relative importance of cross-frontal exchange versus air–sea interaction: McCartney (1977, hereafter MC77) proposed a linkage of new AAIW with the Subantarctic Mode Water (SAMW) in the southeast Pacific and specified the formation of SAMW as a subantarctic process without explicit southern sources; another group, including Molinelli (1978, 1981), Georgi (1979), and PG82, argued that sea–air heat losses could not account for the difference between the Atlantic AAIW and the Pacific AAIW, and the source of the Atlantic AAIW is in the PFZ.

Based on property distributions in streamfunction space, our study suggests that the entire Pacific-Atlantic type of AAIW is derived from polar sources, in agreement with Molinelli (1981).

4. Subantarctic mode water

4.1. Circumpolar distribution

SAMW is a well mixed water mass at 300–600 m depth just north of the SAF (MC77). It is identified as a pycnostad below the seasonal thermocline (a layer of potential vorticity minimum).

The PV-minimum layer north of the SAF, as shown in Fig. 10, starts in the southeast Indian Ocean (100°E) and spans the entire Australian and Pacific sectors, with a progressive cooling and freshening to the east. The deep portion in the southwest Atlantic, however, is at the same depth as the salinity minimum layer (see Fig. 6a) and should be identified as AAIW. This was also pointed out by McCartney (1982).

A plan view on isobaric surface is given in Fig. 11. The low-PV waters at 500 dbar are located in the South Pacific and the South Australia Basin, separated in the Indian Ocean sector by the spreading of high-PV waters from the north. Dissolved oxygen, an independent tracer, displays a similar pattern.

In MC77, SAMW was implied as a continuous water mass circumpolarly advected by the ACC, which may lead to confusion since locations of various fronts were not well-defined in that study. The warm-type mode waters ($\theta > 12^{\circ}$C) in the South Atlantic and the South Indian Ocean (his Fig. 1) are situated north of the Subtropical Front (STF) and should belong to the Subtropical Mode Water (STMW). The STF location can be identified by 10–12°C isotherms at 100 m (O95).

Latter studies by McCartney (1982) and PG82 (also see Fig. 4 in BG96 and Plate 5.4.3 in Hanawa and Talley, 2001) suggest there is little SAMW formation in the South Atlantic and the southwest Indian Ocean, agreeing with our streamfunction analysis. Note that the circumpolar GEM fields do not include STMW ($\phi_{1000} > 1.2$ dyn m).

4.2. Formation mechanism

The formation of SAMW is generally ascribed to late winter convection, a vertical thermodynamic process forced by air–sea fluxes. In this scenario the PV-minimum layer should be exposed to the atmosphere in winter. Fig. 11c shows that the PV-minimum in the southeast Pacific shifts entirely into the PFZ at 200 dbar, suggesting a meridional connection rather than a vertical one.

The connection is obvious in a cross-stream section view (Fig. 3). As discussed earlier, the subduction of the PFZ surface water contributes to the Pacific AAIW. The upper half of the AAIW is nearly isohaline and corresponds to a potential vorticity minimum. Therefore in the southeast Pacific AAIW and SAMW are close (but not identical) and are both formed by along-isopycnal subduction of polar surface waters. In hydrographic surveys, Molinelli (1978) and Gordon et al. (1977) also noticed the thick isohaline layer in the Subantarctic Zone which originated from nearby polar surface waters.

MC77 argued that the cooling and freshening of SAMW to the east is due to large excess of precipitation over evaporation and heat loss to the atmosphere in the Subantarctic Zone. Although

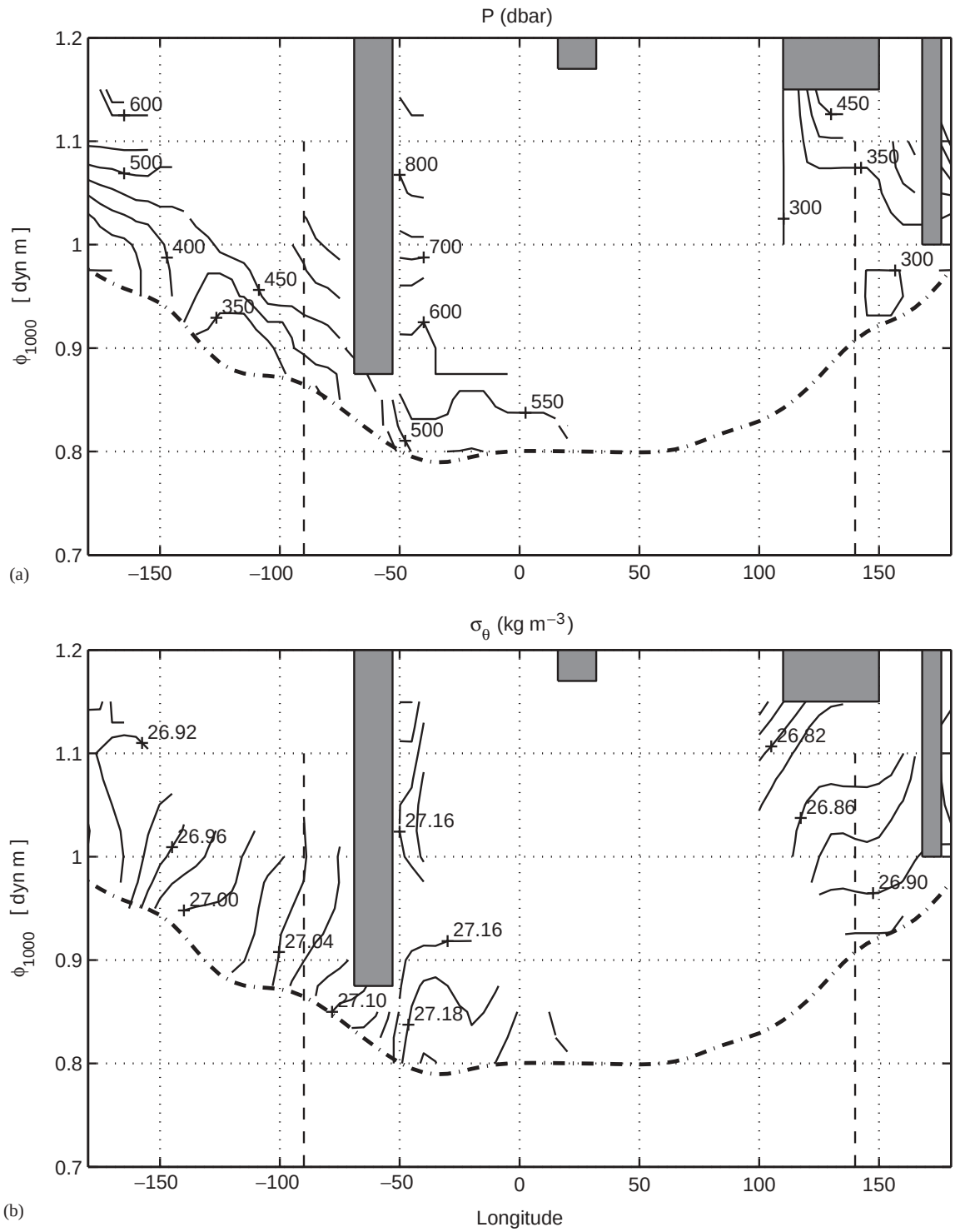

Fig. 10. Core layer view of the PV-minimum layer: (a) pressure, (b) potential density, (c) salinity, and (d) potential temperature.

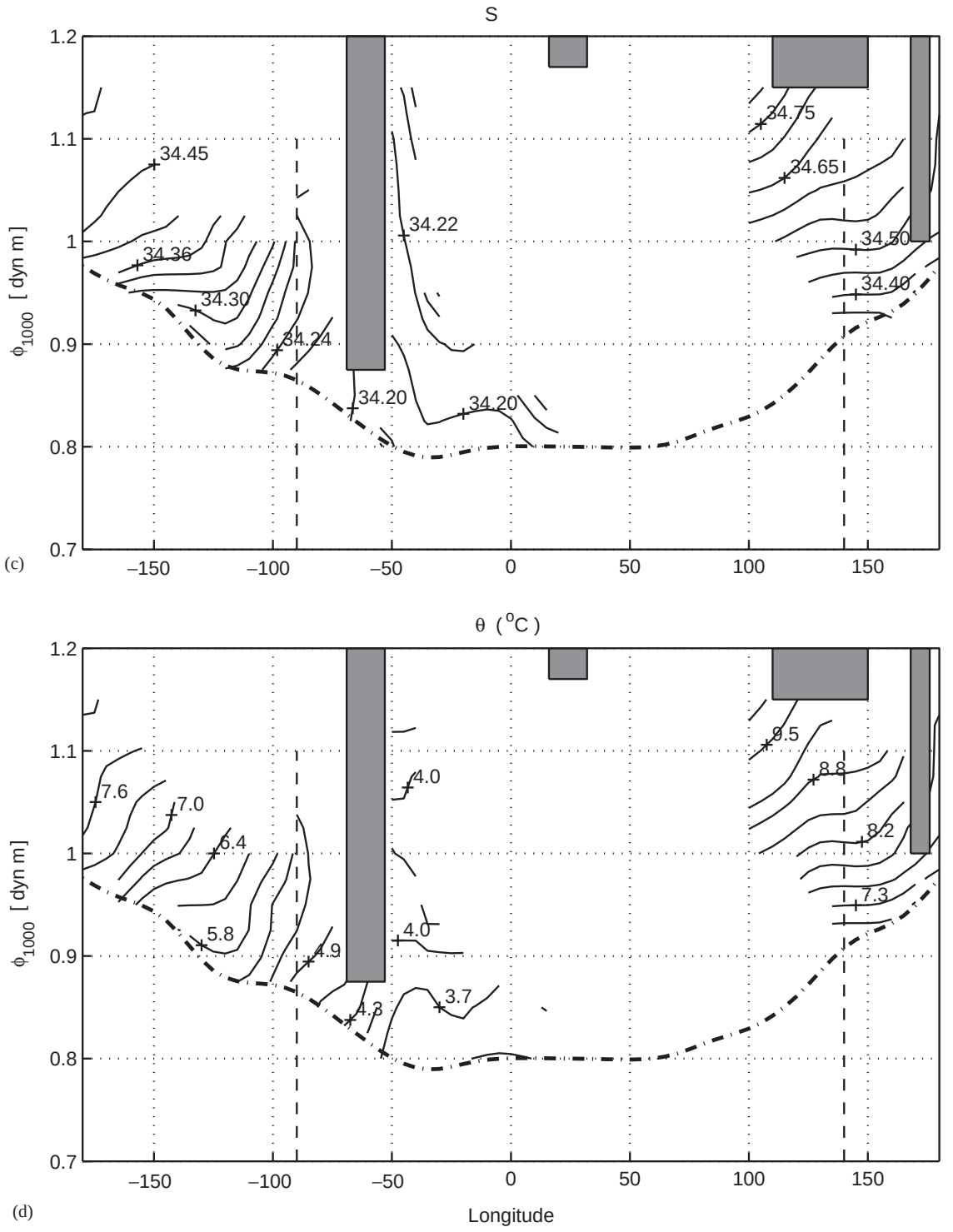

Fig. 10 (*continued*).

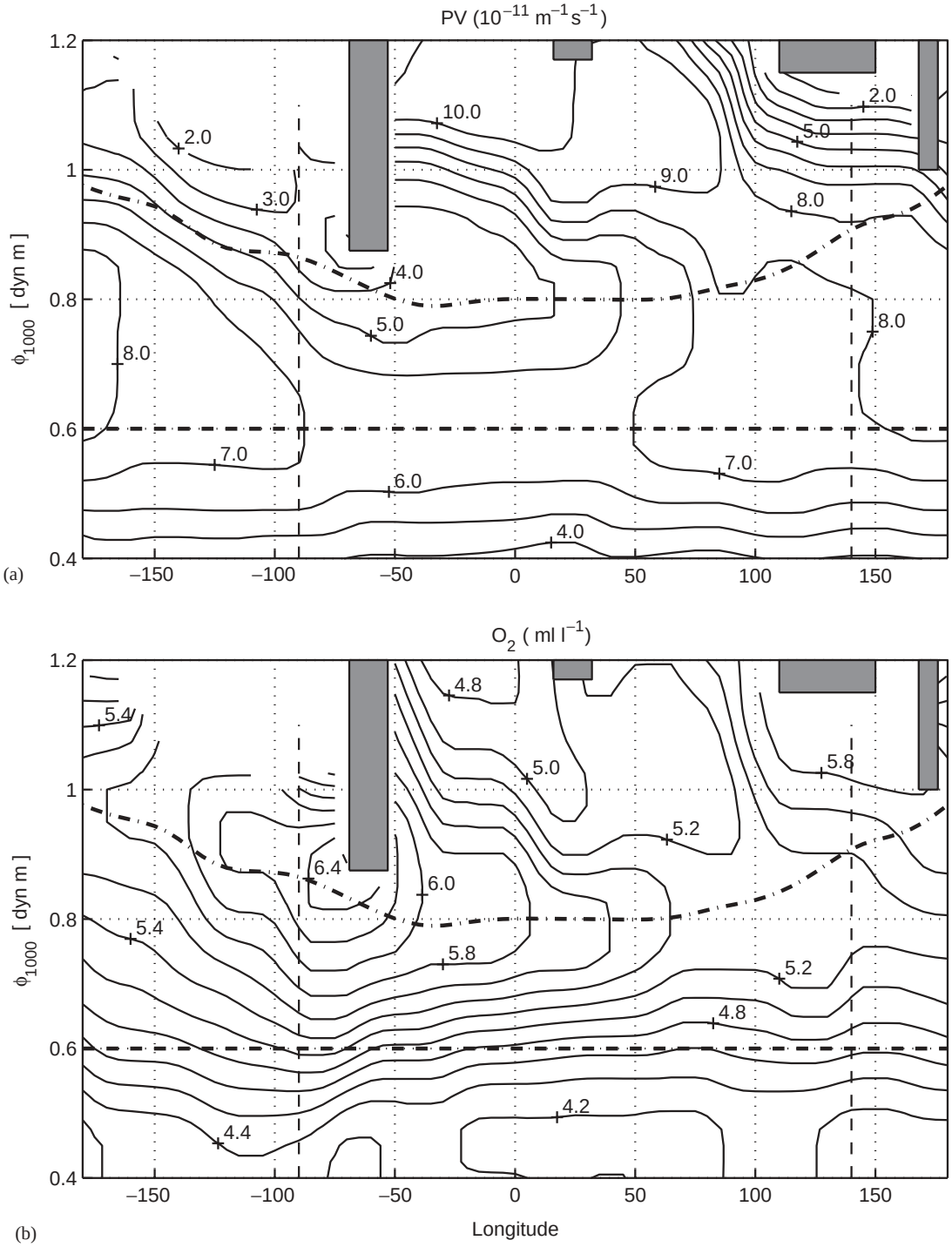

Fig. 11. Plan view of property distribution: (a) potential vorticity at 500 dbar, (b) oxygen at 500 dbar, and (c) potential vorticity in cold season at 200 dbar.

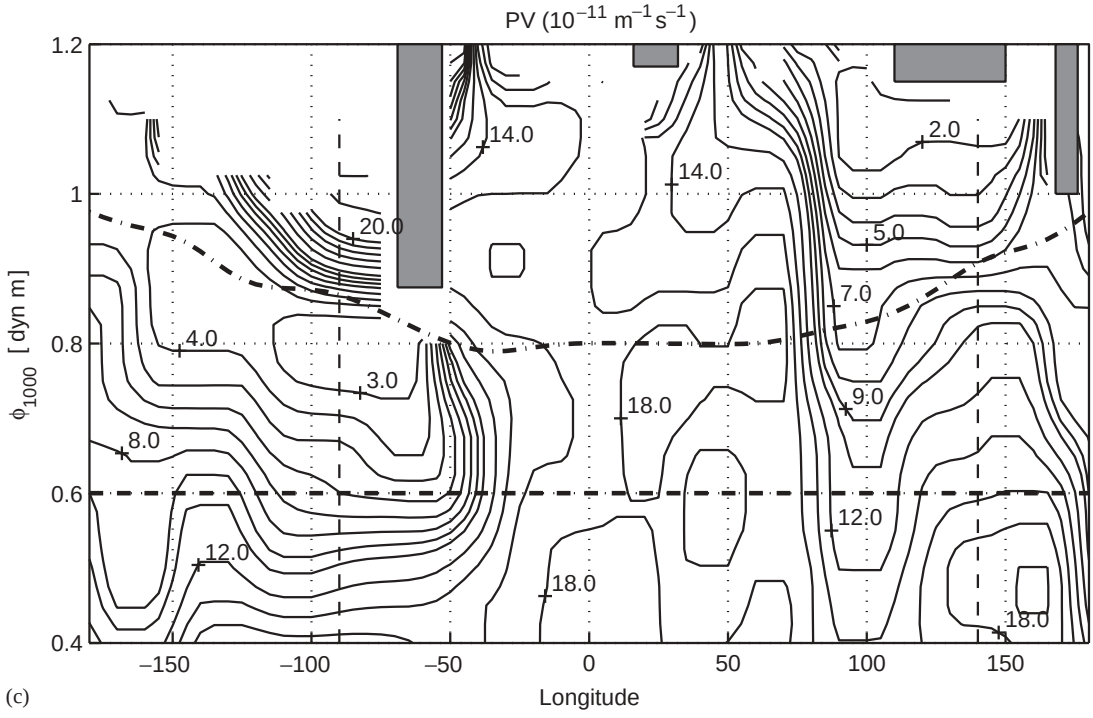

Fig. 11 (*continued*).

we do not exclude air–sea interaction as a factor, the phenomenon is well explained by the subduction of polar surface waters in the southeast Pacific. Ekman transport across the SAF should also play an important role.

4.3. An along-stream view

Fig. 12 shows the property distribution along the SAF (0.06 dyn m north of the SAF axis in Fig. 6). The core of high-PV waters in the Atlantic and Indian sectors gradually descends to 1000 dbar. It sits below a PV-minimum layer in the South Pacific which is derived from polar surface waters. This demonstrates again that AAIW, as defined by the salinity minimum layer, comprises different sources of water in different ACC sectors: the Pacific-Atlantic AAIW contains southern sources and tends to follow the 27.1 kg m^{-3} isopycnal; the Indian–Australian AAIW sits on the 27.2 kg m^{-3} isopycnal and is strongly modified by the Agulhas water from the north.

In Fig. 12 the freshening and cooling of SAMW in the South Pacific is deep-reaching (down to 1000 dbar), appearing to support the modification by meridional processes rather than air–sea fluxes in the Subantarctic Zone. A following study will use dynamic analysis to directly relate water mass formation to large-scale overturning motions in the Southern Ocean.

Acknowledgements

A discussion with Dr. Igor Belkin on structural criteria and mode water distribution was helpful. Comments from Drs. Peter Cornillon, John Merrill and two anonymous reviewers are appreciated. The GEM analysis is based on a historical dataset compiled by the Alfred Wegener Institute. The SAFDE project is funded by the National

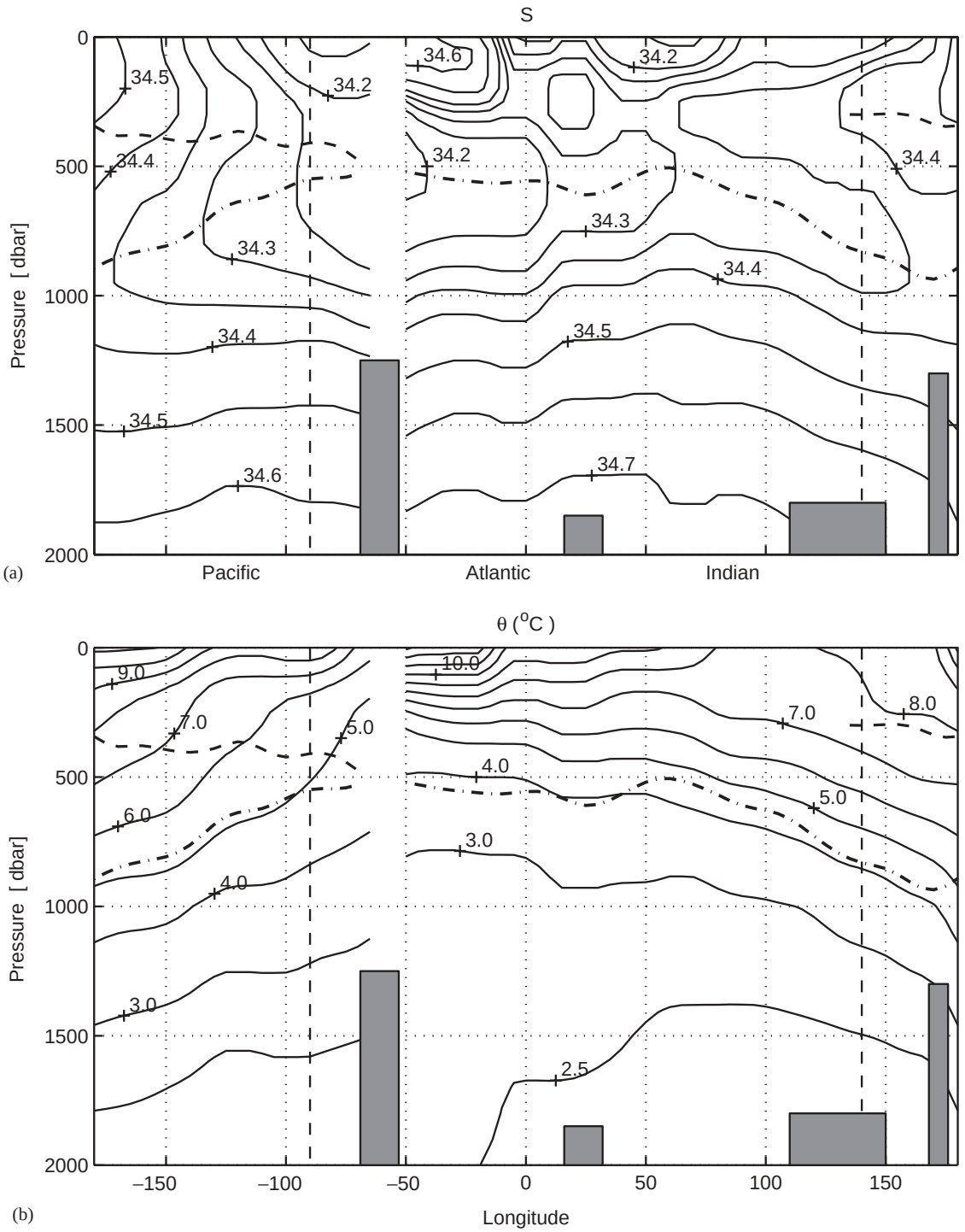

Fig. 12. Along-stream view of GEM fields at 0.06 dyn m north of the SAF. The dash-dotted curve represents the core of the salinity minimum layer. The dashed curve represents the core of the PV-minimum layer.

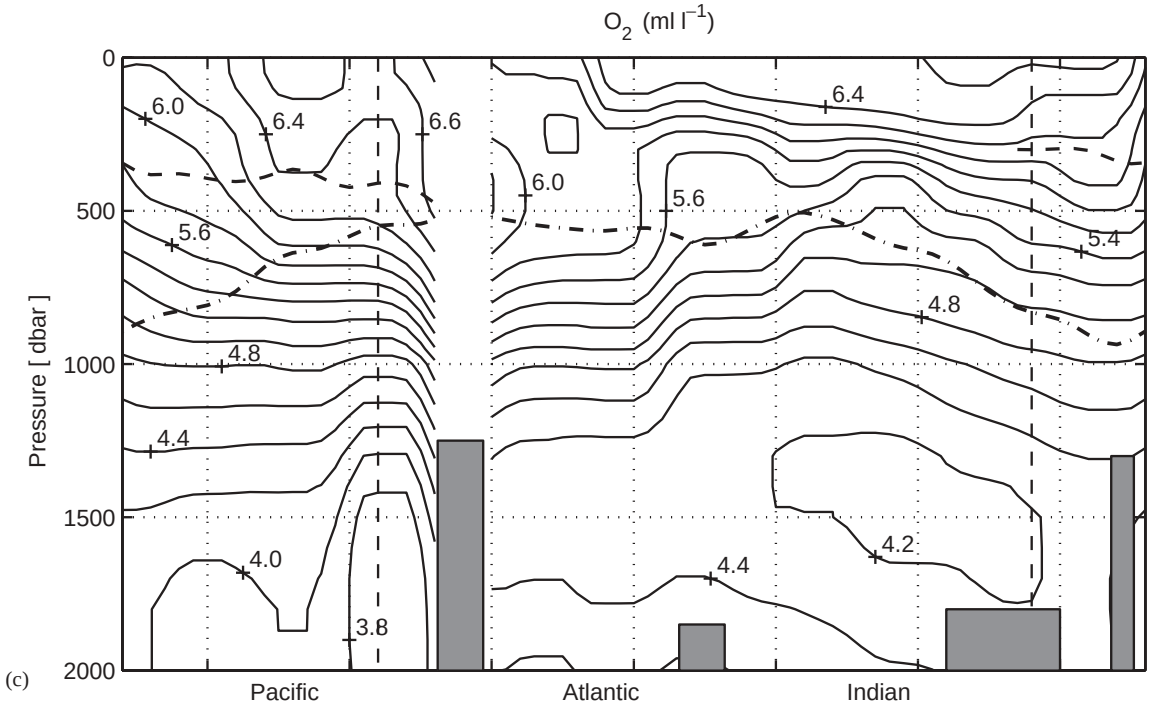

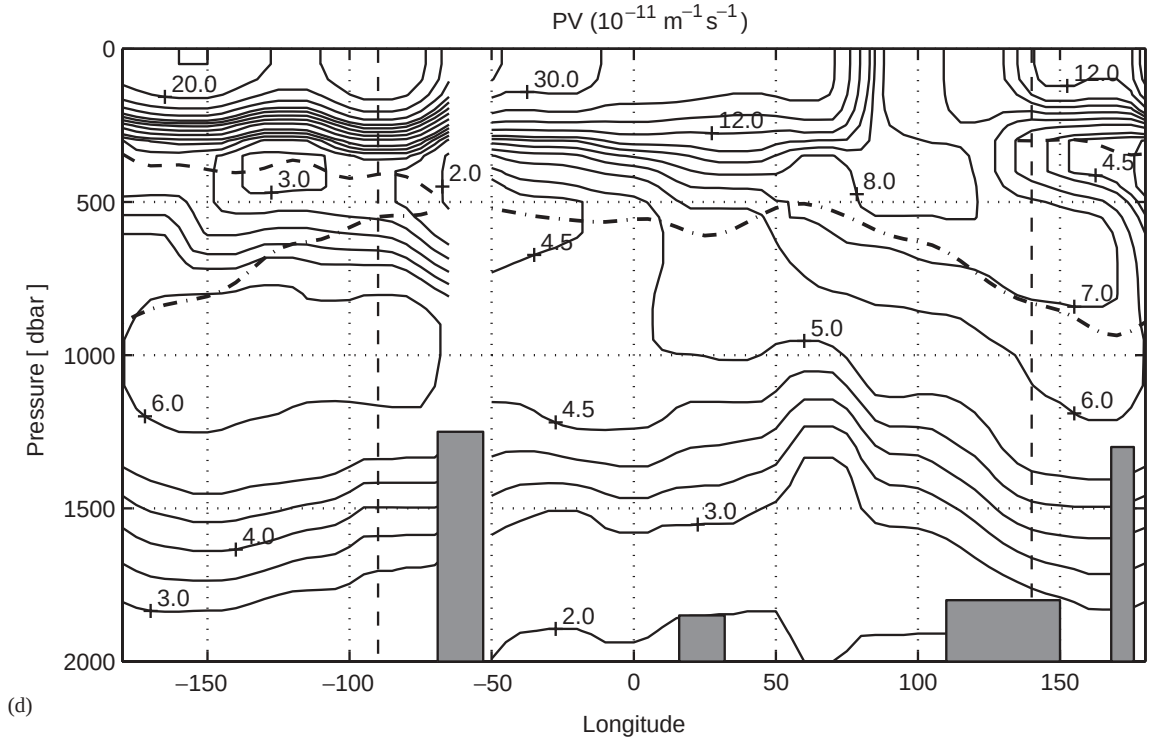

Fig. 12 (*continued*).

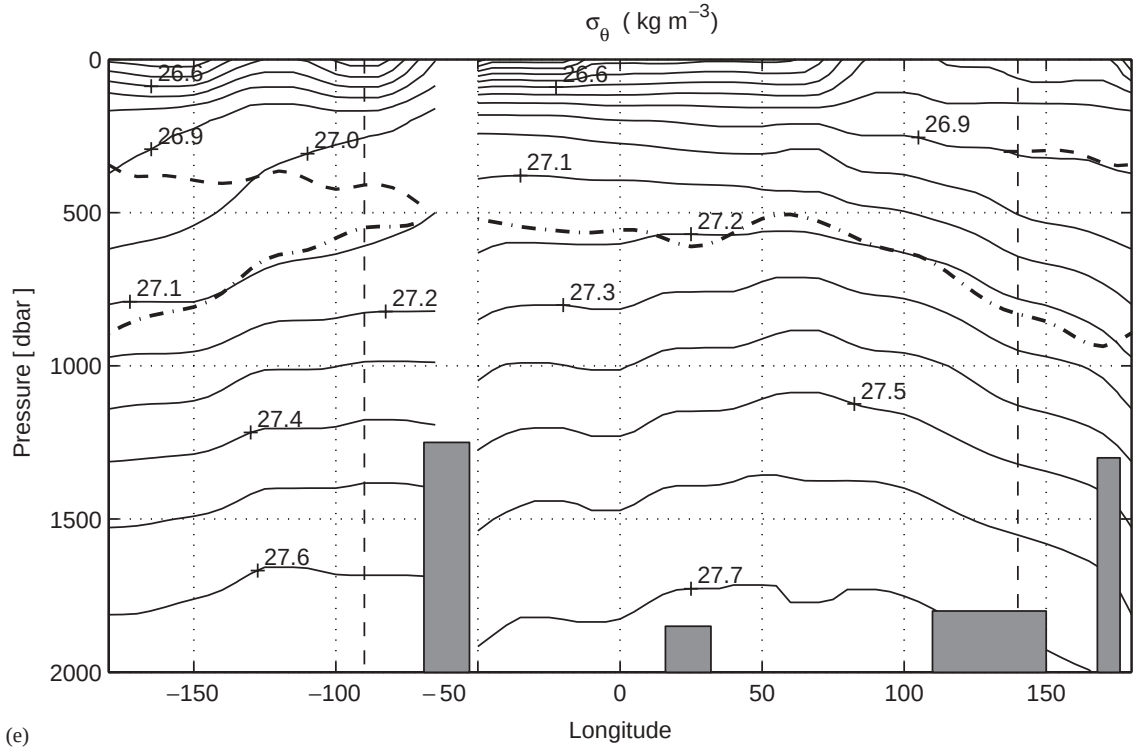

Fig. 12 (*continued*).

Science Foundation under Grants OCE-92-04041 and OCE-99-12320. The first author was recently supported by the Visiting Scientist Program at GFDL/NOAA.

References

Belkin, I.M., Gordon, A.L., 1996. Southern Ocean fronts from the Greenwich meridian to Tasmania. Journal of Geophysical Research 101, 3675–3696.

Burling, R.W., 1961. Hydrology of circumpolar waters south of New Zealand. New Zealand Department of Scientific and Industrial Research Bulletin 143, 66pp.

Georgi, D.T., 1979. Modal properties of Antarctic intermediate water in the Southeast Pacific and the South Atlantic. Journal of Physical Oceanography 9, 456–468.

Gill, A.E., 1982. Atmosphere-Ocean Dynamics. Academic press, New York, 662pp.

Gordon, A.L., Georgi, D.T., Taylor, H.W., 1977. Antarctic Polar Front Zone in the western Scotia Sea. Journal of Physical Oceanography 7, 309–328.

Hanawa, K., Talley, L.D., 2001. Mode waters. In: Siedler, G. (Ed.), Ocean Circulation and Climate. Academic Press, New York, pp. 715.

McCartney, M.S., 1977. Subantarctic Mode Water, In: Angel, M. (Ed.), A Voyage of Discovery, Deep-Sea Research 24, 103–119.

McCartney, M.S., 1982. The subtropical recirculation of mode waters. Journal of Marine Research 40, 427–464.

Molinelli, E., 1978. Isohaline thermoclines in the Southeast Pacific Ocean. Journal of Physical Oceanography 8, 1139–1145.

Molinelli, E., 1981. The Antarctic influence on Antarctic intermediate water. Journal of Marine Research 39, 267–293.

Nowlin Jr., W.D., Whitworth III, T., Pillsbury, R.D., 1977. Structure and transport of the Antarctic Circumpolar Current at Drake Passage from short term measurements. Journal of Physical Oceanography 7, 788–802.

Orsi, A.H., Whitworth III, T., Nowlin Jr., W.D., 1995. On the meridional extent and fronts of the Antarctic Circumpolar Current. Deep-Sea Research I 42, 641–673.

Piola, A.R., Georgi, D.T., 1982. Circumpolar properties of Antarctic intermediate water and Subantarctic Mode Water. Deep-Sea Research 29, 687–711.

Peterson, R.G., Whitworth III, T., 1989. The Subantarctic and Polar Fronts in relation to deep water masses through the southwestern Atlantic. Journal of Geophysical Research 94, 10817–10838.

Rintoul, S.R., Donguy, J.R., Roemmich, D.H., 1997. Seasonal evolution of upper ocean thermal structure between Tasmania and Antarctic. Deep-Sea Research I 44, 1185–1202.

Sievers, H.A., Nowlin Jr., W.D., 1984. The stratification and water masses at Drake Passage. Journal of Geophysical Research 89, 10489–10514.

Sun, C., 2001. The columnar structure in stratified geostrophic flows. Geophysical and Astrophysical Fluid Dynamics 95, 55–65.

Sun, C., Watts, D.R., 2001. A circumpolar gravest empirical mode for the Southern Ocean hydrography. Journal of Geophysical Research 106, 2833–2856.

Sun, C., Watts, D.R., 2002. A pulsation mode in the Antarctic Circumpolar Current south of Australia. Journal of Physical Oceanography 32, 1459–1479.

Sun, C., Watts, D.R. The heat flux carried by the ACC mean flow. Journal of Geophysical Research, in press.

Talley, L.D., 1996. Antarctic intermediate water circulation in the South Atlantic. In: Wefer, G. (Ed.), The South Atlantic: Present and Past Circulation. Springer, Berlin, pp. 219–238.

Watts, D.R., Sun, C., Rintoul, S.R., 2001. A two-dimensional gravest empirical modes determined from hydrographic observations in the Subantarctic Front. Journal of Physical Oceanography 31, 2186–2209.

Whitworth III, T., Nowlin Jr., W.D., 1987. Water masses and currents of the Southern Ocean at the Greenwich meridian. Journal of Geophysical Research 92, 6462–6476.